

Authors response to Anonymous Referee #2

Major comments:

1. **(Comment)** This manuscript introduces a technique for describing cloud processes using the drop size distribution gamma fit coefficients, and the trajectory of these coefficients in three-dimensional space. Comparisons within this phase space are made among clouds with different environmental conditions and linked to various cloud processes. While the manuscript is well written, I think some aspects of the paper need further work.

1. **(Answer)** We thank Anonymous Referee #2 for the invaluable comments. Please find in this document the detailed responses to your concerns.

2. **(Comment)** First, the physical insights that are provided are not closely linked to the coefficients themselves, and instead are reworked into pseudo-forces related to condensation and collision processes. However, the method used to decompose the trajectories into these pseudo forces is not clearly described, and as a result I find it difficult to accept many of the explanations behind the patterns in the data.

2. **(Answer)** Indeed, the pseudo-forces presented are somewhat loosely defined, which is one of the main reasons why we use “Illustration of microphysical processes...” in the title. The use of the Gamma phase space as an entity is new to the microphysical studies and we do not aim to cover all its aspects in this first introduction. We are already working in a new study focusing only on cloud modeling to extract the pseudo-forces definition and to show how this approach can be useful for microphysical modeling. In this study, our main interest is to show that we can study patterns in this space and that it can be useful to the tools already implemented in models (or remote sensing applications) and to develop new ones.

That said, we followed your suggestion and dedicated efforts to better define and quantify the pseudo-forces properties. We identified that the ideal tool to address this issue would be a relatively simple model that solves the condensation and collision-coalescence growth using the bin approach instead of the bulk. A model that fits those requirements is described in Feingold et al. (1999) – item “c” in section 3, where we run only two parcels and not a bigger ensemble. This is a parcel model that treats the DSDs in 35 mass-doubling bins from 3.5 μm up to ~ 9 mm in diameter. The processes solved by the model are: 1) CCN activation, considered to be composed of ammonium sulfate; 2) growth by condensation; 3) growth by collision-coalescence and 4) effects of giant CCN on the DSD evolution (we turn this process off for the purposes of this review). Other processes such as aqueous chemistry, complex aerosol composition, trace gases and radiation (and the effects of those processes on the DSDs) are not treated. Additionally, by being a parcel model, it does not consider turbulent mixing and sedimentation from above.

The characteristics of the model make it suitable to simulate the effects of condensation and collision-coalescence growth in the DSDs, which we can use to show the related patterns in the

Gamma phase-space. We tried to produce results based on the conditions measured during flight AC09 (now RA1), where we used the following parameters as input: 1) mean aerosol diameter $D_g = 1.55 \mu\text{m}$, with standard deviation of 2.2 for the lognormal function of the aerosols; 2) pressure at cloud base of 890 hPa; and 3) temperature at cloud base of 20.85 °C. The vertical speed was fixed at 0.5 m s^{-1} as we wanted to minimize the effect of new droplet formation in the DSD shape. Under those conditions, we ran the model twice: one run with only condensational growth (CG run) and one with both condensation and collision-coalescence growth (C2G run). Both runs produced the exact same DSDs in the lower parts of the cloud where the condensation dominates, but differed significantly when the collision-coalescence became active (around 1200 m, where cloud base is at 0 m). When the collision-coalescence process activates, $D_{\text{eff}} \approx 25 \mu\text{m}$ and the condensational growth is much less effective. Therefore, it was possible to isolate both processes. Because there is no turbulent mixing or dilution with dry air, the droplet growth with altitude is much more pronounced in the model compared to our measurements during AC09. For this reason, we do not limit the Gamma fit to $D < 50 \mu\text{m}$ as in the paper. Otherwise, it would be difficult to capture the effects of the collision-coalescence process – droplets grow relatively quickly beyond the 50 μm mark.

We fitted Gamma DSDs (using the same moments of order zero, two, and three as in the paper) to the model outputs every 20 seconds. Therefore, each point in the Gamma phase space represents the instantaneous DSD measured every 20 seconds. The results are shown in the following three figures.

Figure R1 shows the Gamma phase space for both runs, where “*” markers are related to CG run and squares to C2G. The arrows represent the displacement vector every 20 seconds, which is related to the respective pseudo-force (colors represent altitude above cloud base in m). Note that in the first 500 m the Gamma points are the same for both runs. This layer is defined by condensational growth alone and we observe a “zig-zag” pattern in the Gamma phase-space. When the trajectory is upwards in the “zig-zag”, they are similar to what we observed in the paper – that is, growing μ and Λ (and shrinking N_0) along with the condensational growth. On the other hand, the model results also show a downward (in the Gamma space) trend during condensational growth. We noted that when the trajectory is downwards, the Gamma fit does not represent the DSD width correctly. At those points, the fixed bins between 10 μm and 15 μm present fast-growing concentrations (when the droplets grow sufficiently to transition from the lower bins) that disproportionately affects the Gamma DSD width. In the downward pattern, the Gamma DSD relative dispersion can be up to 150% higher than the binned DSD. When the process stabilizes, the trajectory returns to the upward trend and the Gamma and binned DSD widths get progressively closer (~20% to ~50% difference). Based in those results we can conclude that the condensational growth in the model produces trajectories in similar directions to what we observed in the paper.

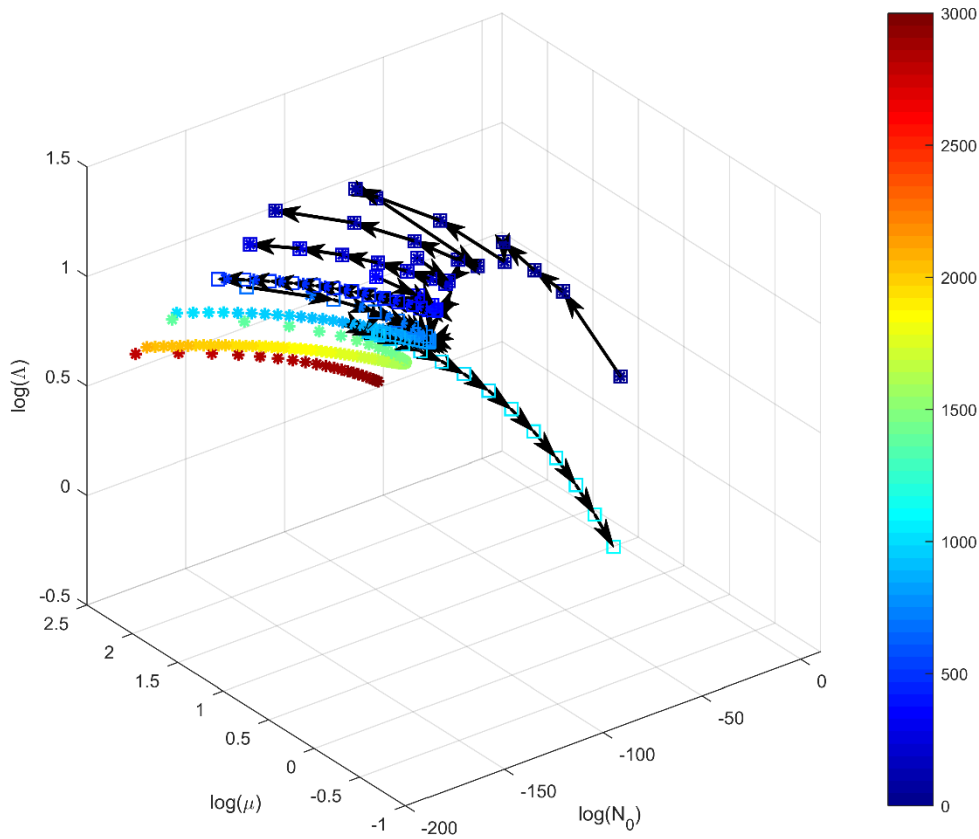


Figure R1: Gamma phase-space for both CG and C2G runs. The “*” markers are relative to the CG run, while squares represent the C2G run. Arrows represent the displacement vector between each 20-s point, which is related to the respective pseudo-force. Colors represent altitude above cloud base in m.

Figure R2 shows the same points of Figure R1, but colored according to D_{eff} . Additionally, we show lines of constant D_{eff} along a surface (not shown) of $N_d = 250 \text{ cm}^{-3}$ similarly to Figure 10 in the paper. The lines start at $5 \mu\text{m}$ in the top and grow in $5 \mu\text{m}$ intervals up to $50 \mu\text{m}$ in the bottom line. When comparing the trajectories with the D_{eff} lines, it is possible to see where the droplets are growing faster. For instance, the condensational growth close to cloud base is very effective (because the droplets are smaller) and the trajectory tend to cross the D_{eff} lines. However, when droplets reach $D_{\text{eff}} \approx 25 \mu\text{m}$, the trajectories get almost parallel to the lines, showing slower growth. On the other hand, the collisional growth accelerates with increasing D_{eff} . This is expected from theory, but it is interesting to quantify its effects on the spherical coordinates of the displacement vectors – Figure R3.

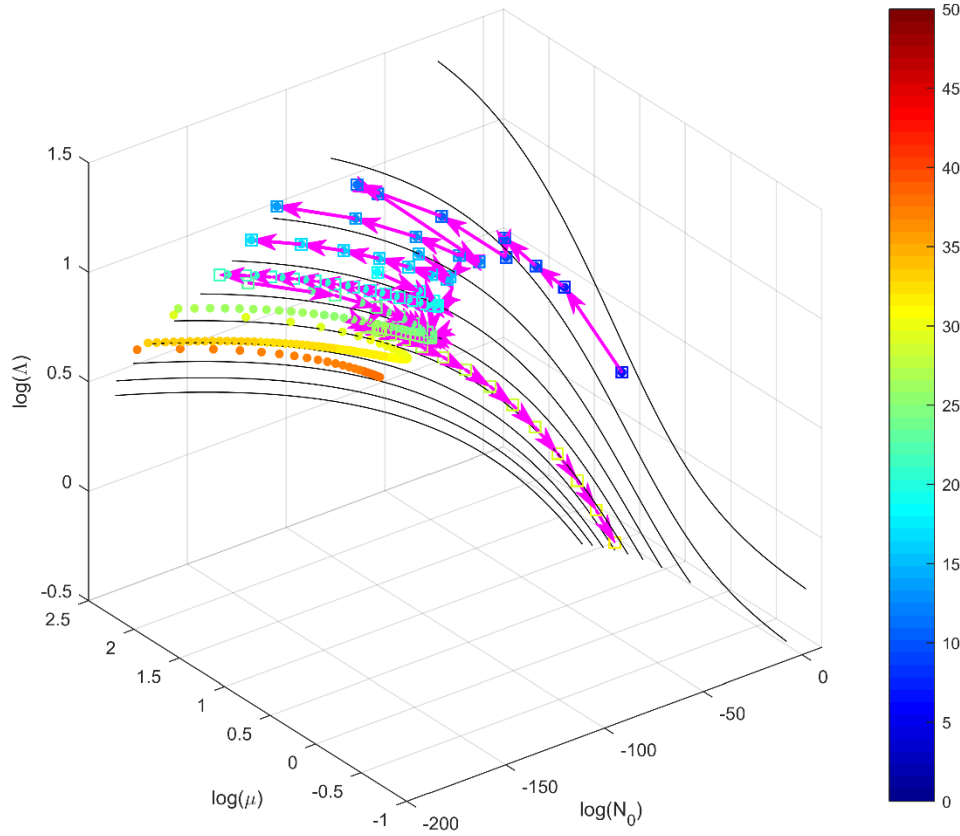


Figure R2: similar to Figure R1, but colored according to D_{eff} . The lines shown are lines of constant D_{eff} along a surface of $N_d = 250 \text{ cm}^{-3}$ as in Figure 10 in the paper, going from $5 \mu\text{m}$ (top line) to $50 \mu\text{m}$ (bottom line) – $5 \mu\text{m}$ intervals.

Figure R3 shows the spherical coordinates of the vectors in Figures R1 and R2. θ is the azimuth angle measured in the plane $\log(N_0) \times \log(\mu)$, being 0 at the $\log(N_0)$ axis and growing counter-clockwise. ϕ is the elevation angle, measured from the plane $\log(N_0) \times \log(\mu)$ to the $\log(\Lambda)$ axis. The size of the vectors is measured by r . In Figure R3 we excluded the points in the downward part of the “zig-zag” mentioned above. Non-filled circles in Figure R3 represent condensational growth alone, while filled markers represent collision-coalescence (colors are altitude above cloud base in m). It is possible to note that the elevation angle ϕ is slightly positive for the condensational growth, decaying with D_{eff} . The average value of this angle is 0.26° . It has small values mainly because of the bigger values of $\log(N_0)$ as compared to $\log(\Lambda)$. Nonetheless, the most important feature is its sign transition from condensational to collisional growth. On the latter, the angle seems to grow linearly with D_{eff} (except for the last point) as the process intensifies – averaged value of -4.23° . Overall, this angle is related to the DSD curvature trend – positive when the curvature is shrinking (condensational growth) and negative when the curvature is increasing (collisional growth).

The azimuth angle θ defines how N_0 and μ evolve along the trajectory. For the condensational growth, this angle averages 179.6° , meaning growing $\log(\mu)$ and shrinking $\log(N_0)$. On the other hand, this angle averages -13.7° for collisional growth and results in the opposite trend for the parameters. Both observations are in line with what we observed in the paper – now there is at

least some quantification of the angles. Note that the angles most likely have different values in our observations given the differences in the values of the Gamma parameters. However, their sign, and therefore the direction of the motion in the space, is the same between our model calculations and the observations shown in the paper. Finally, we can note that r tends to decrease as the condensation rates decay, but it does not increase as the collisional growth intensifies. However, the acceleration of the collisional growth is reflected in ϕ and θ – both decrease, resulting in a trajectory that crosses the D_{eff} lines in Figure R2.

Overall, the modeling results presented here clearly indicate that the patterns observed in the Gamma phase space in the paper are indeed related to the condensation and collision-coalescence processes. The relation between both processes and the evolution of the Gamma parameters are consistent between the Lagrangian simulation and the observations. The natural next step would be to calculate the speeds and accelerations (and therefore the actual pseudo-forces), but this will not be addressed in this introduction paper. The actual implementation of the concepts presented here would need further work that is beyond the scope of the present study. A study is underway using different parametrizations, aerosol properties and environmental properties.

We added three new paragraphs to Section 2.3 commenting on the Lagrangian model results and detailed it a little more in the supplement (with the figures/text shown here for the readers).

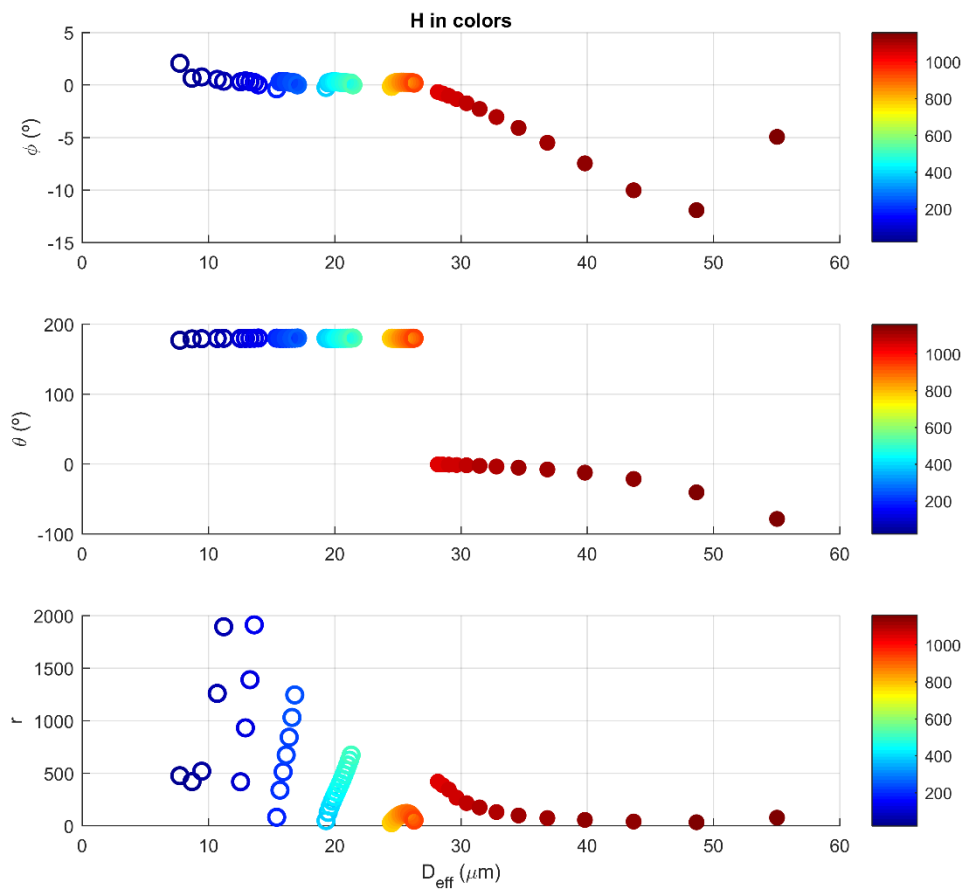


Figure R3: spherical coordinates of the displacement vectors shown in Figures R1 and R2. θ is the azimuth angle in the $\log(N_0) \times \log(\mu)$ plane, growing counter-clockwise (is 0 at the $\log(N_0)$)

axis). ϕ is the elevation angle from the $\log(N_0) \times \log(\mu)$ towards the $\log(\Lambda)$ axis and r is the size of the vectors. The colors represent altitude above cloud base in m.

3. **(Comment)** Secondly, gamma functions often provide good mathematical fits to drop size distributions, but attempting to understand cloud processes using the fit coefficients is fraught with difficulty, which I don't think is addressed sufficiently in this manuscript. Gamma function coefficients can vary substantially depending on the fit method used, the size range over which the fit is made, and the suitability of the underlying size distribution shape to be fit with a gamma. Many of these issues were addressed in the recent publication by McFarquhar et al. (JAS 2014). Using different fitting methods they found that the N_0 coefficient, for example, can vary by many orders of magnitude, even when the same moments (1, 2, and 6) are used to make the fit. Using a different set of moments, like the 0th, 2nd, and 3rd used in this manuscript would likely result in even larger changes. Furthermore, the coefficients N_0 and μ are inextricably linked, with N_0 having the units of $m^{-(4-\mu)}$. So as μ changes, N_0 will respond mathematically, even though such a change may not represent a physical process.

3. **(Answer)** The Gamma function and its parameters are indeed complex to use in practical applications. Additionally, the N_0 , μ , and Λ parameters can sometimes seem as abstract numbers that are mathematically loosely defined. In other words, those parameters can have extreme behaviors depending on the way you choose to calculate them. However, their values and, perhaps most importantly, their interdependence is singular in each methodology. For instance, we could have different values for the Gamma parameters shown in the paper and the spherical coordinates shown in Figure R3 if we were to use, say, moments 3, 4, and 6 for the fit. If we were to compare between the two methodologies, it wouldn't be a fair comparison because their internal functioning (i.e. their parameter space) is different. Fits that use higher-order moments have stronger weights for bigger droplets, affecting the parameters values and their phase space. What we can do is to fix in a particular methodology and make the pattern analysis inside its particular phase space. We specifically chose to use moments 0, 2, and 3 in order to obtain a parameter space that is similar to what a bulk model should be able to reproduce. With regards to the moment method, we believe this is the best approach given that it precisely reproduces at least 2 moments predicted by bulk models (e.g. droplet number concentration and liquid water mixing ratio).

When the methodology is fixed, it doesn't really matter if, for instance, N_0 covers several orders of magnitude. In our modeling calculations N_0 went from $\sim 10^{-150}$ to $\sim 10^1$, but all those values are inside the phase space and can be expected when the DSDs fit certain criteria. We noted that N_0 reach such low values for narrower DSDs, like the ones that appear after long periods of (exclusively) condensational growth. Therefore, the theoretical phase space allows for such wide variability. The observations, on the other hand, will of course cover a much more limited volume in the phase space. The idea is that both theoretical and observed phase spaces operate under the same underlying "laws" – at least considering only condensation and collision-coalescence growth, the model should be expanded to encompass other processes.

Regarding the linkage between N_0 and μ : as you correctly pointed out, those parameters are mathematically linked by definition. In fact, all three parameters are correlated in one way or another. When you go back to the equations used to obtain the parameters, this is very clear:

first you obtain μ as a function of a dimensionless ratio between the moments, then you obtain Λ from μ , and finally N_0 from both of them. The relation between the Gamma parameters, modulated by the three moments, is a key aspect that generates the trajectories observed. If the parameters were completely independent, there wouldn't be trajectories in the phase space. There would probably be "clusters" of points for various types of DSDs. Our methodology aims to take advantage of this relationship in order to help on pattern recognition. It follows that the phase space is non-orthogonal, where it can "shrink" or "inflate" depending on the region of analysis. This is possibly one of the difficulties in applying this method to models, because the mathematic deductions are not straightforward. However, the ability to describe the microphysical evolution in this space opens new possibilities for DSD modeling, potentially improving subsequent calculations such as evaporation, sedimentation, etc.

I understand that the relationship between μ and N_0 is mathematical, but I would like to point out that it also makes physical sense. Take Equation 9 from the paper:

$$\varepsilon = \frac{\sigma}{D_g} = \frac{1}{\sqrt{\mu + 1}}$$

This equation states that the relative dispersion (or DSD width) can be calculated directly from μ . When μ increases, the DSD gets narrower. In that case, the left tail of the DSD gets closer to the maximum concentration diameter. Therefore, the intercept has to be lower and N_0 also shrinks. If you consider condensational growth, the situation is the same – see figures here and in the paper. Therefore, the linkage between N_0 and μ also have association to physical processes. When we look at the collision-coalescence growth, the opposite happens - μ decreases causing N_0 to increase.

4. **(Comment)** A more effective method may be to plot the moments themselves in 3D space rather than first fitting them to a gamma function. The moments are more easily linked to known microphysical processes, and if they are computed directly from the distributions do not suffer from the complications of poor fitting. The moments can always be computed from modeled DSDs as well, which would the avoid the further complications introduced when models use restricted gamma parameter spaces. At the very least, I think the authors should investigate the sensitivity of the observed phase-space patterns to different gamma fitting methods, and more clearly identify the source and interpretation of the F_{cd} and F_{cl} pseudo-forces.

4. **(Answer)** We believe that plotting the moments in a 3D space would be very similar to plotting the Gamma parameters. The moments are also not independent, thus resulting in a similar non-orthogonal space. However, the linkage between the moments-space and the underlying DSD is non-trivial. You would need to apply transformations to obtain the respective DSDs. Therefore, we believe the Gamma phase-space is more suitable in order to be portable for other applications. Also, as commented above, some calculations explicitly need the DSD parameters.

Regarding other methods to fit the DSDs, we tested a new fit based on moments of order 3, 4, and 6 (M346). Here we reproduce Figures R1-3 with this new approach (Figures R4-6). For this case, we had to limit the fittings to $D < 150 \mu\text{m}$ because of the stronger weight to bigger droplets that caused negative values of μ . Note that the patterns in the phase-space are very similar to

the previous case (M023). Averaged values for θ and ϕ are 179.5° and 0.35° for condensation and -19.4° and -4.0° for collision-coalescence, respectively.

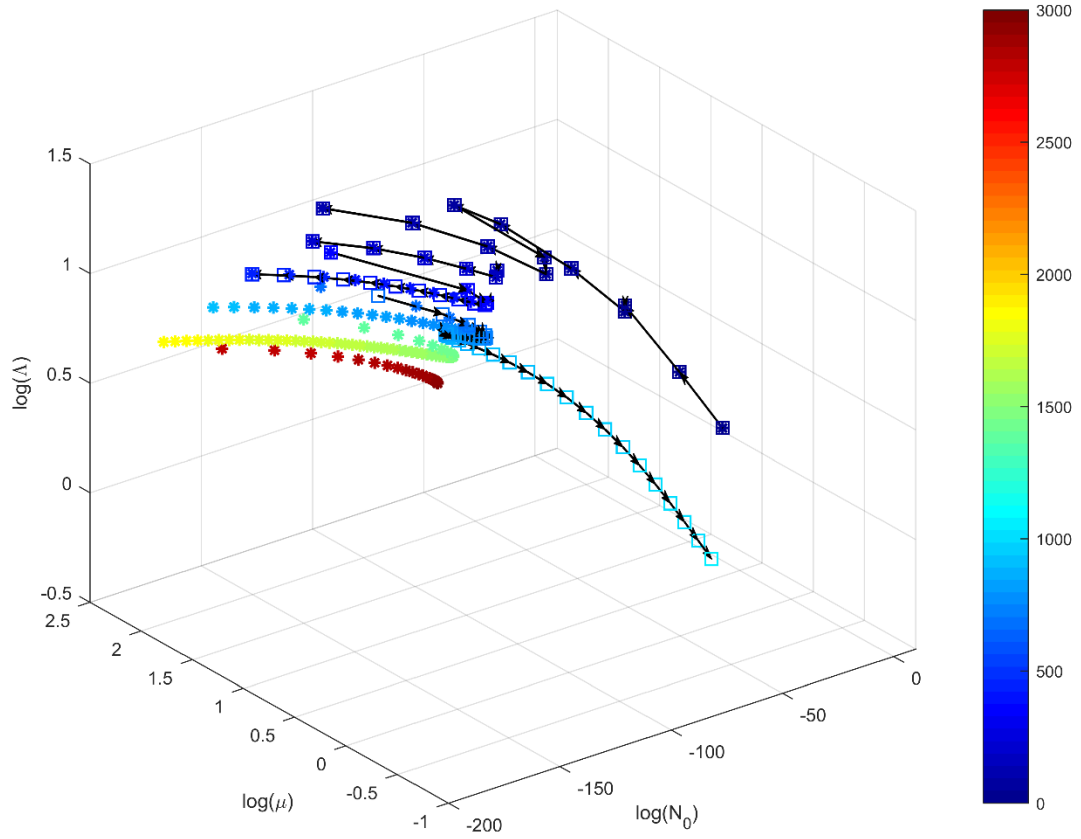


Figure R4: same as Figure R1, but for M346.

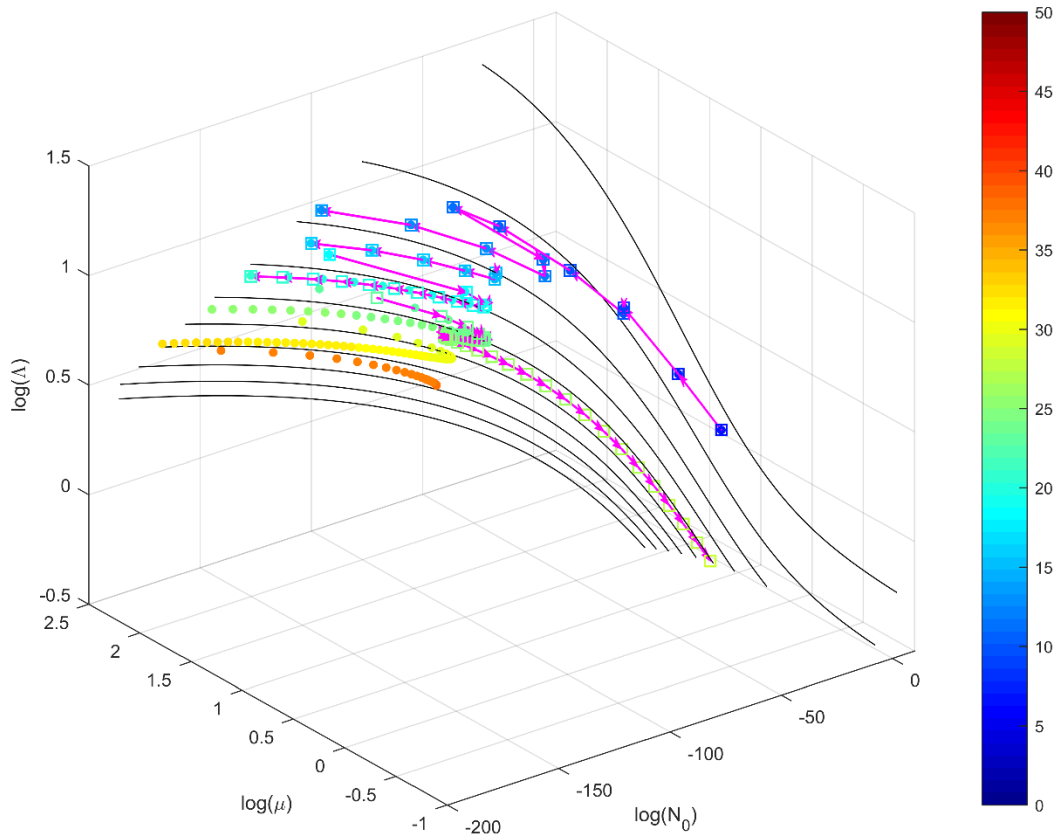


Figure R5: same as Figure R2, but for M346.

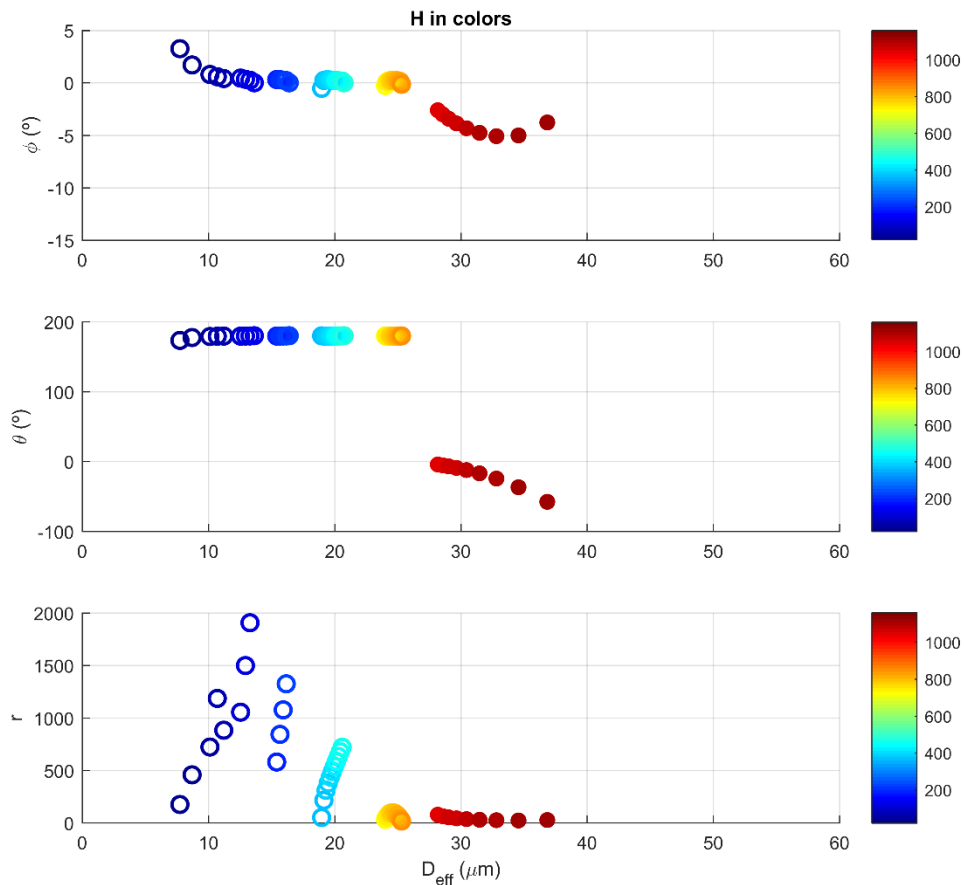


Figure R6: same as Figure R3, but for M346.

Specific comments:

1. **(Comment)** Section 2.2: How were DSD shapes that are not well fit by a gamma function handled in the analysis (e.g. bimodal or skewed distributions)?

1. **(Answer)** No special routine was applied to bimodal or skewed distributions. The idea is to produce the phase-space of the observations as is (except for the filter to remove residual DSDs) within the limitations of the Gamma fit.

2. **(Comment)** Section 2.3: The introduction of the F_{cd} and F_{cl} pseudo-forces seem incomplete and leaves many unanswered question, such as: How were they determined, i.e. can they be presented mathematically? Do they completely describe the total force F ? Are they orthogonal, if not, in which direction in the phase space does each force point?

2. **(Answer)** Please refer to our answer to your major comments and the new paragraphs in Section 2.3.

3. **(Comment)** Figures 3,5,6,7, and 8: It is difficult to determine where the lines and points are in 3-D space. A projection of the fit lines onto the X, Y, and Z planes would greatly help with the visualization.

3. **(Answer)** We left Figure 3 as is for simplicity, but added the requested projections to the other figures.

4. **(Comment)** Section 2.3: Given the sensitivity of N_0 to the μ parameter, the speculations regarding N_0 would be much more convincing if N_d (or 0th moment) were used instead.

4. **(Answer)** Our affirmations about N_0 were not speculations, but based on our measurements – note that the trajectories shown in Figures 5-8 point out to the patterns commented in Section 2.3. The new model calculations also corroborate our affirmations.

5. **(Comment)** Section 3.2: The manuscript states that measurements were taken ‘close to cloud top’, but more information is needed about the placement of the measurements in the cloud. Was the aircraft making multiple passes to a fixed location, or attempting to intercept the same visual position in the cloud on multiple passes? How long did the aircraft pattern take relative to the lifetime of the cloud, and at what point in the life cycle of the cloud were the measurements taken?

5. **(Answer)** We added the following sentences to Section 2.1 to clarify the flight strategy: “The latter step was deployed as follows. After the cloud base penetration, the aircraft performed several penetrations in vertical steps of several hundred meters. In each step, the aircraft penetrated the cloud tops available, thus avoiding precipitation from above. In this way, different clouds can be penetrated in the same altitude level, but the vertical steps followed the growing cumuli field overall”.

6. **(Comment)** Section 3.3: How were the clean and polluted clouds determined? Were the flight patterns and environmental conditions for each of these clouds comparable?

6. **(Answer)** The clean and polluted clouds were determined based on the measurements shown in Table 1 – i.e. the aerosol concentrations. All flight patterns followed the steps we described in Section 2.1 and we also show them in the map in Figure 1. The environmental conditions are discussed in Figure 4 and Table 1.